

Two-Phase Flow Behavior in Microtube Reactors During Biodiesel Production from Waste Cooking Oil

Guoqing Guan, Marion Teshima, Chie Sato, Sung Mo Son,
Muhammad Faisal Irfan, and Katsuki Kusakabe

Dept. of Living Environmental Science, Fukuoka Women's University, 1-1-1 Kasumigaoka,
Higashi-ku, Fukuoka 813-8529, Japan

Norihiro Ikeda

Dept. of Environmental Science, Fukuoka Women's University, 1-1-1 Kasumigaoka,
Higashi-ku, Fukuoka 813-8529, Japan

Tsao-Jin Lin

Dept. of Chemical Engineering, National Chung Cheng University, Min-Hsiung, Chia-Yi, Taiwan

DOI 10.1002/aic.12042

Published online September 25, 2009 in Wiley InterScience (www.interscience.wiley.com).

Flow patterns in the course of transesterification of waste cooking oil (WCO), sunflower oil (SFO) with water and/or oleic acid as a model of WCO, and pure SFO in the presence of a KOH catalyst in microtubes were investigated. FAME yield for the transesterification of WCO reached more than 89% in the microtube reactors with a residence time of 252 s at 333 K. The flow patterns when using WCO were changed from a liquid–liquid slug flow at the inlet region to a parallel flow at the middle region, and then to a homogeneous liquid flow at the outlet region as the reaction proceeded at 333 K. Fine droplets containing glycerol and methanol generally formed in oil slugs when using pure SFO, but were almost unobservable when using WCO. The soap produced from free fatty acids was considered to be the main factor affecting the flow patterns of WCO and SFO. © 2009 American Institute of Chemical Engineers AIChE J, 56: 1383–1390, 2010

Keywords: biodiesel fuel, two-phase flow, microreactor, transesterification, droplets

Introduction

Microchannel reactors have many advantages over conventional reactors, including great improvement in reaction rate and product yield, energy efficiency, and on-site/on-demand production.^{1–3} The reaction between immiscible

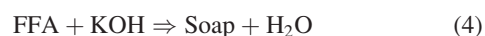
liquids can be enhanced by using a slug-flow microchannel reactor.^{4–12} Transesterification of vegetable oil with methanol to produce biodiesel fuels (BDF) is a typical two-phase reaction. To improve the mass transfer between the two phases, vigorous agitation is needed in a conventional batch reactor.^{13–15} Recently, it was suggested that a microreactor was suitable for use in the transesterification of vegetable oil in the production of BDF.^{16–20} It was reported that the required reaction time was remarkably reduced when a microreactor was used instead of a batch reactor, suggesting that mass transfer across the boundary of immiscible liquids in a

Correspondence concerning this article should be addressed to K. Kusakabe at kusakabe@fww.ac.jp

Current Address of Guoqing Guan: Institute of Industrial Science, The University of Tokyo, 4-6-1 Komaba, Meguro-ku, Tokyo 153-8505, Japan

microchannel could be significantly enhanced. The complex interaction between the two immiscible phases during the transesterification of sunflower oil (SFO) with methanol was characterized by using a transparent FEP microtube reactor in our previous study.²¹ Fine droplets containing the produced glycerol and methanol formed at the interface between oil and methanol phases, and then moved into the oil slugs. Fine glycerol-methanol droplets formed in the oil slugs were attributed to the existence of diglyceride and monoglyceride produced at the beginning of transesterification, which served as an emulsifier to stabilize the surface of the formed droplets.

In this study, waste cooking oil (WCO), SFO with water and/or oleic acid as a model of WCO, and pure SFO were used as the feedstock of BDF. The flow patterns in the microchannel were investigated. WCO contains a large amount of free fatty acids (FFA) and water. In this case, the following reactions should be considered when using the alkaline catalyst.



The reaction mixture is composed of TG, methanol, DG, MG, FAME, GL, H₂O, soap, and catalyst. Therefore, the flow patterns may be different when using pure SFO. This study has three objectives: (1) to characterize the flow patterns when using different feedstock; (2) to investigate the interface phenomena in order to explain the flow pattern transitions; and (3) to examine the relationship between flow patterns and FAME yield.

Experimental

Chemicals

WCO was provided from a biodiesel production factory. SFO for use in cooking was purchased. Dehydrated methanol, potassium hydroxide, oleic acid, glycerol, acetic acid, and phloxine B were obtained from Wako Pure Chemical Ind. Ltd., Japan. The acid and saponification values of the oil were determined using standard titration methods.²² The molecular weight of the oil was determined from the saponification and acid values. Water content in the oil was determined using a Karl-Fischer moisture titrator (MKC-610, Kyoto Electronic Manufacturing). The viscosity was determined with a torsion-balanced, oscillation-type viscometer (VM-1G, CBC Materials). The density was determined using a density meter (DA-130N, Kyoto Electronic Manufacturing). The physical properties of the oils are summarized in Table 1. According to the contents of water and FFA in the WCO, SFO was adjusted to be an oil mixture containing either 0.8 wt % H₂O, or 6.6 wt % oleic acid, or both. When FFA is assumed to be composed of oleic acid, an acid

Table 1. Physical Properties of WCO and Sunflower oil

	Waste cooking oil	Sunflower Oil
Water content, wt %	0.8	<0.1
Acid value, mgKOH g ⁻¹	13.1	0.41
Saponification value, mgKOH g ⁻¹	233.1	192.4
Molecular weight, g mol ⁻¹	765.2	876.6
Viscosity, mPa s (20°C)	55.6	62.1
Density, g cm ⁻³ (25°C)	0.92	0.91

value of 13.1 mg KOH g⁻¹ corresponds to 6.6 wt% of oleic acid.

Observation of flow patterns

Transparent PTFE tubes with a diameter of 0.46, 0.68, 0.86, and 0.96 mm were used for the transesterification reaction and for observation of flow patterns. The experimental setup has been described elsewhere.²¹ To obtain clear images of the flow patterns in the microtube, a 4.5 wt % methanol solution of KOH was dyed with inert red phloxine B. Red phloxine B is soluble in glycerol, but is insoluble in oil. The transparent PTFE tube with a length of 800 mm fixed onto a silicone rubber plate was placed on a hot plate. A transparent glass plate closely covered the microtube for prevention of heat loss. Syringe pumps were used to feed the oil and methanol. They were mixed at a T-shaped joint before entering the microtube reactor. For the 0.96 mm microtube, the total flow rate was fixed at $2.3 \times 10^{-6} \text{ mm}^3 \text{ s}^{-1}$, corresponding to a residence time of 252 s. To standardize the residence time in different microtubes, total flow rates for 0.86, 0.68, and 0.46 mm microtubes were fixed at 1.8×10^{-6} , 1.1×10^{-6} , and $5.3 \times 10^{-7} \text{ mm}^3 \text{ s}^{-1}$, respectively. The flow rate of methanol with KOH was equal to that of oil. The reaction temperatures were fixed at 40 and 60°C. Pictures of the microtube were taken with a digital single-lens reflex camera. Details of the flow behavior in the microtube were observed and recorded using an optical microscope equipped with a digital camera. The shutter speed was 1/40 s.

The change of the interface tension in the oil during the methanol phase at 298 K was observed using the pendant drop technique.^{23,24} Methanol or a 4.5 wt % methanol solution of KOH was used to fill a rectangular pyrex cell (10 mm × 10 mm × 45 mm). The temperature was controlled at exactly 25°C. Using an injection glass needle with a diameter of 0.9 mm, the oil was slowly introduced into the methanol phase and a single drop was formed on the tip of the needle. The change in the shape of the oil drop on the tip of the glass needle was observed with the reaction time noted, a pictures were taken automatically every 30 s. Apparent interfacial tension was determined from the characteristic length of an oil drop and by the density difference between the oil and the methanol phase. The volume of the drop was evaluated from the maximum diameter of a drop, assuming that its shape was a sphere.

Determination of FAME yield

The transesterification was carried out at 313 and 333 K, and the methanol and oil flow rates were the same. At a point 200, 400, or 800 mm from the inlet, the microtube was

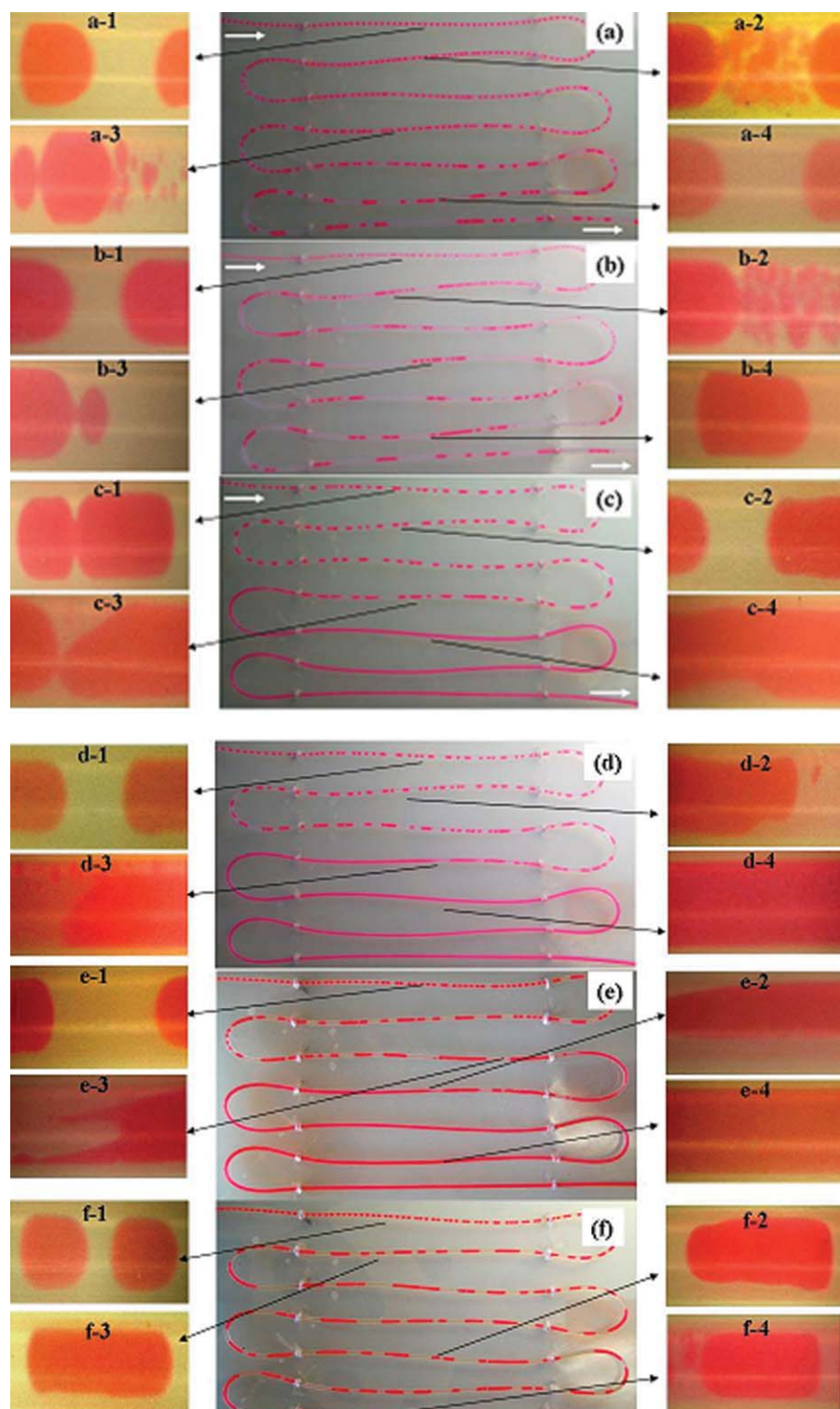


Figure 1. Two-phase behaviors in a microtube reactor with a diameter of 0.96 mm when using oils with different compositions: (a) SFO (333 K); (b) SFO + 0.8 wt % H₂O (333 K); (c) SFO + 6.6 wt % oleic acid (333 K); (d) SFO + 0.8 wt % H₂O + 6.6 wt % oleic acid (333 K); (e) WCO (333 K); (f) WCO (313 K).

Oil flow rate = $1.15 \times 10^{-6} \text{ mm}^3 \text{ s}^{-1}$; methanol flow rate = $1.15 \times 10^{-6} \text{ mm}^3 \text{ s}^{-1}$. [Color figure can be viewed in the online issue, which is available at www.interscience.wiley.com.]

connected to an acetic acid solution line for the termination of the reaction, and the sample was collected at each point. The sample was then centrifuged at 6000 rpm for 1200 s.

The upper FAME layer was washed several times with deionized water to remove residual inorganic components. Then, $1 \times 10^{-4} \text{ mm}^3$ of the washed sample was diluted in 3

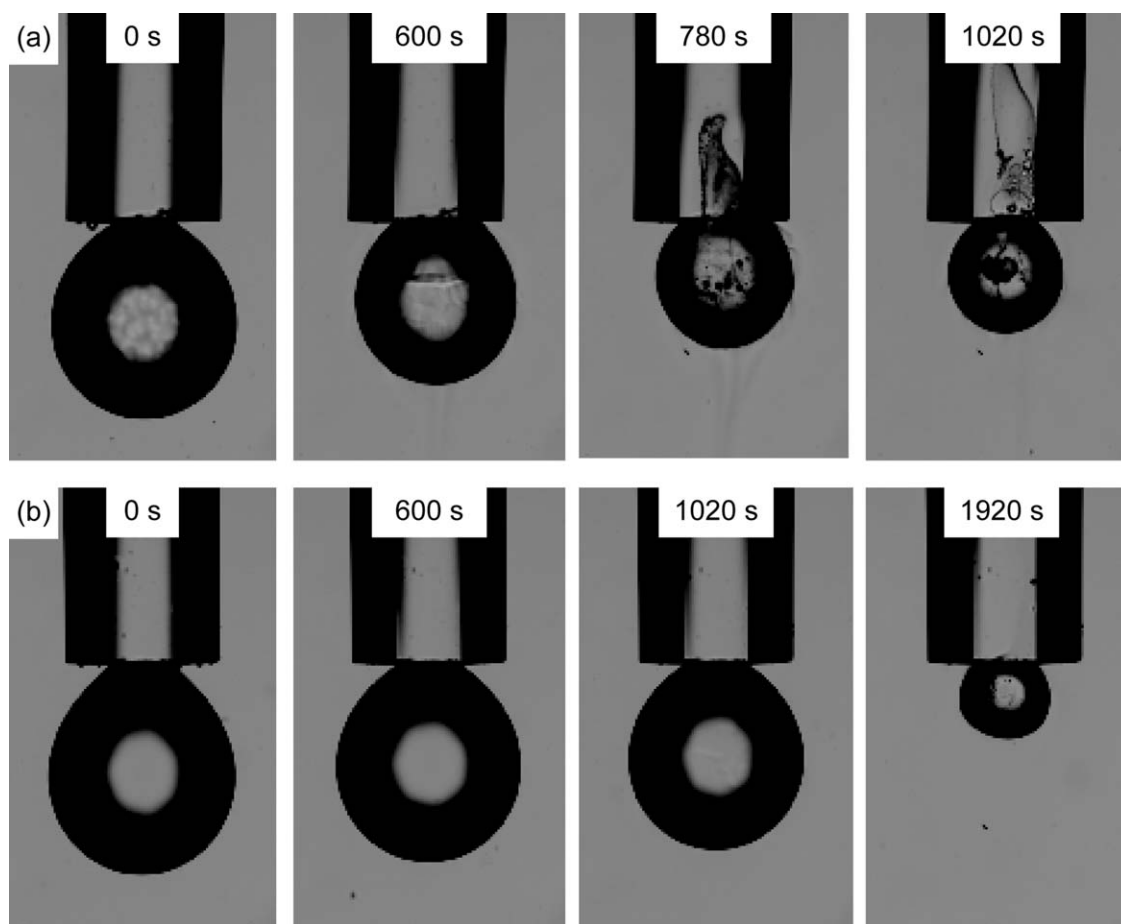


Figure 2. The shape change of oil drop in 4.5 wt % KOH-methanol phase at 298 K. (a) SFO, (b) WCO.

$\times 10^{-3} \text{ mm}^3$ of hexane for analysis. The concentration of unreacted oil that remained in the sample was analyzed using a high-performance liquid chromatograph (HPLC, Tosoh Corp.) equipped with a silica-gel column (Shimpack CLC-SIL, Shimadzu Corp.) and a refractive index detector. The mobile phase was *n*-hexane/2-propanol = 99.5/0.5 (v/v) and the column temperature was kept constant at 313 K. Two peaks that were attributed to the sum of FAMES and the unreacted glycerides (sum of mono-, di-, and tri-glycerides) appeared in the liquid chromatogram. The FAME yield in the product was calculated as follows:

$$\text{FAME yield} = \frac{C_{\text{FAME}}}{3C_{\text{oil}}} \times 100 \quad (6)$$

where C_{oil} and C_{FAME} are the concentrations of triglycerides in the inlet and FAME in the product, respectively.

Results and Discussion

Figure 1 shows the flow patterns when different oil feed-stock was used in a PTFE microtube with a diameter of 0.96 mm. The total flow rates were fixed at $2.3 \times 10^{-6} \text{ mm}^3 \text{ s}^{-1}$, and the flow rate of methanol with KOH was equal to that of oil. As shown in Figures 1a, b, the flow patterns in the cases of either SFO or SFO with 0.8 wt % water were

similar. Clear stable segments (a-1 and b-1 in Figure 1) in the microtube were formed in the inlet region. Then red fine droplets (a-2 and b-2 in Figure 1), which were composed mainly of glycerol and methanol,²¹ were observed forming in the oil slugs, and their fraction was increased along the flow direction. In the middle region, the aggregation of the formed fine droplets was enhanced due to the internal circulation flow and large droplets formed in the oil slug (a-3 and b-3 in Figure 1). In the outlet region, the aggregated droplets in the oil phase almost completely merged into the methanol phase and disappeared (a-4 and b-4 in Figure 1). However, the coalescence of segments seemed simple in the presence of water, as shown in Figure 1b. In our previous study,²¹ a FEP microtube was used, and the fine droplets formed in the oil segments were formed in a similar manner, but the segmented flow was converted to a quasi-homogeneous one in the exit region of the microtube when using pure SFO. However, the same phenomena were not observed when using a PTFE tube, suggesting that the surface properties of a microtube could strongly affect the flow patterns, but, it had no effect on the formation of fine droplets in the oil segments.

The flow pattern in the case of WCO (Figure 1e) was similar to those of SFO with 6.6 wt % oleic acid (Figure 1c) and to the SFO with 6.6 wt % oleic acid plus 0.8 wt % water (Figure 3d). Flow patterns of the separated oil and methanol phases in the inlet region could also be seen (d-1

and e-1 in Figure 1), but slug aggregation (c-1 in Figure 1) also occurred in this region. In the middle parts along the flow direction, the coalescence became vigorous, but no fine droplets appeared in the oil segments from the inlet to the middle regions (c-2, c-3, and d-2 in Figure 1). Simultaneously, the shape of some slugs began to deform (c-3, d-3, e-2, and e-3 in Figure 1). For WCO, the separated slug flows could easily become parallel (e-2 in Figure 1).

In order to clear the interface phenomena, an oil droplet in the methanol containing 4.5 wt % of KOH were observed at 298 K. As shown in Figure 2, the drop size of SFO and WCO decreased as the reaction proceeded. FAME produced by the transesterification could dissolve in methanol and oil. Glycerol is soluble in FAME and oil to a negligible extent, but is completely soluble in methanol.^{25–27} The produced FAME and glycerol on the interface could diffuse into methanol, resulting in shrinkage of the oil drop. In the case of SFO, fine droplets could be observed in the oil drop at 780 s, then the fine droplet size in the oil drop increased with the reaction time. After a reaction of 1020 s, the grown-up droplets inside the oil drop fell into the methanol by gravitational force, resulting in a sharp decrease in the volume of the oil drop. To the contrary, the shrinkage rate of the WCO drop was smaller than that of the SFO drop, suggesting that the reaction rate was very slow in the presence of FFA. As with the results shown in Figure 1, no fine droplets were observed in the oil phase. Although the environment of the static state was different from that of the flow state in the microtube, the interface change was similar in both cases.

Figures 3a,b show the volume ratio and the apparent interfacial tension of the drop, respectively. The SFO drop initially expanded in the absence of the KOH catalyst due to the diffusion of methanol into the oil phase. In the presence of a KOH catalyst, the drop size of SFO constantly decreased due to the diffusion of FAME and glycerol produced by the transesterification in the methanol phase. On the other hand, the WCO drop size slightly decreased regardless of the existence of the catalyst during the first 600 s of the reaction. This means that the transfer of water and FFA into the methanol phase played an important role regardless of the saponification of FFA, which hindered the progress of the transesterification of TG in the initial period.

The apparent interfacial tensions were calculated by assuming that the densities of the oil drop and methanol phase were constant. The apparent interfacial tensions of the SFO and WCO drops were slightly changed even in the absence of a KOH catalyst, as shown in Figure 3b. The interfacial tension of WCO-methanol containing 4.5 wt % KOH (2.174 mN/m) was ~2 times lower than that of the SFO-methanol (3.991 mN/m) at the beginning of the reaction. The two-phase flow patterns in the microchannel were strongly related to the Capillary and Reynolds numbers and decrease in interfacial tension tended to form parallel flows.⁶ Therefore, in comparison with a SFO-methanol system, the lower interfacial tension in a WCO-methanol system could more easily result in the change from a slug flow to a parallel flow, as shown in e-2 of Figure 1.

As shown in Figure 3b, the interfacial tension of SFO-methanol decreased according to the progress of the transesterification. The reduction in the interfacial tension might

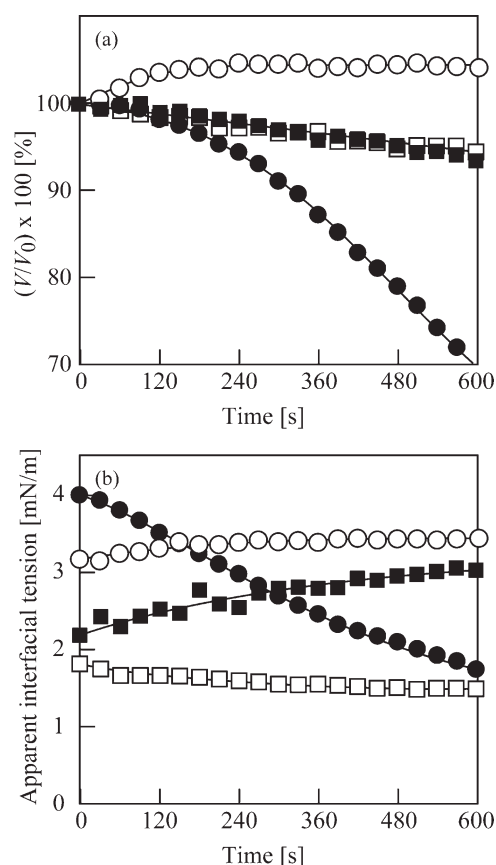


Figure 3. Volume ratio of oil drop (a) and apparent interfacial tension between oil and methanol (b) at 298 K.

●○: SFO-methanol; ■□: WCO-methanol; ●■: 4.5 wt % KOH in methanol; ○□: pure methanol.

have been caused by the formation of DG and MG, which have a higher hydrophilicity than TG. Thus, fine droplets consisting of glycerol and methanol were formed at the interface between the oil and methanol phases due to the stabilization effect of weak surfactants like DG and MG and been dispersed into the oil phase due to the friction caused by the internal flow and the interfacial tension.²¹ Meanwhile, the interfacial tension of WCO-methanol increased with the increase in reaction time. In the first 600 s reaction in the static state, the saponification of FFA was the main reaction, and therefore, the produced fatty acid soap influenced the interfacial phenomena. It was reported that the formed fatty acid soap existed almost completely in the methanol-glycerol phase.²⁶ The interfacial tension of WCO-methanol was lower than that of the SFO-methanol at the beginning of the reaction. This means that the FFA and other impurities in WCO could stabilize the surface, then the fatty acid soap produced by the saponification of FFA on the surface was easily transferred to the methanol phase, resulting in the slight rise in interfacial tension. The high interfacial tension of WCO-methanol after a reaction time of 600 s could prevent the transportation of glycerol and methanol and the formation of their fine droplets in a WCO drop.

As the reaction proceeded, FAME also increased in the reaction system. The formed FAMES served as co-solvents

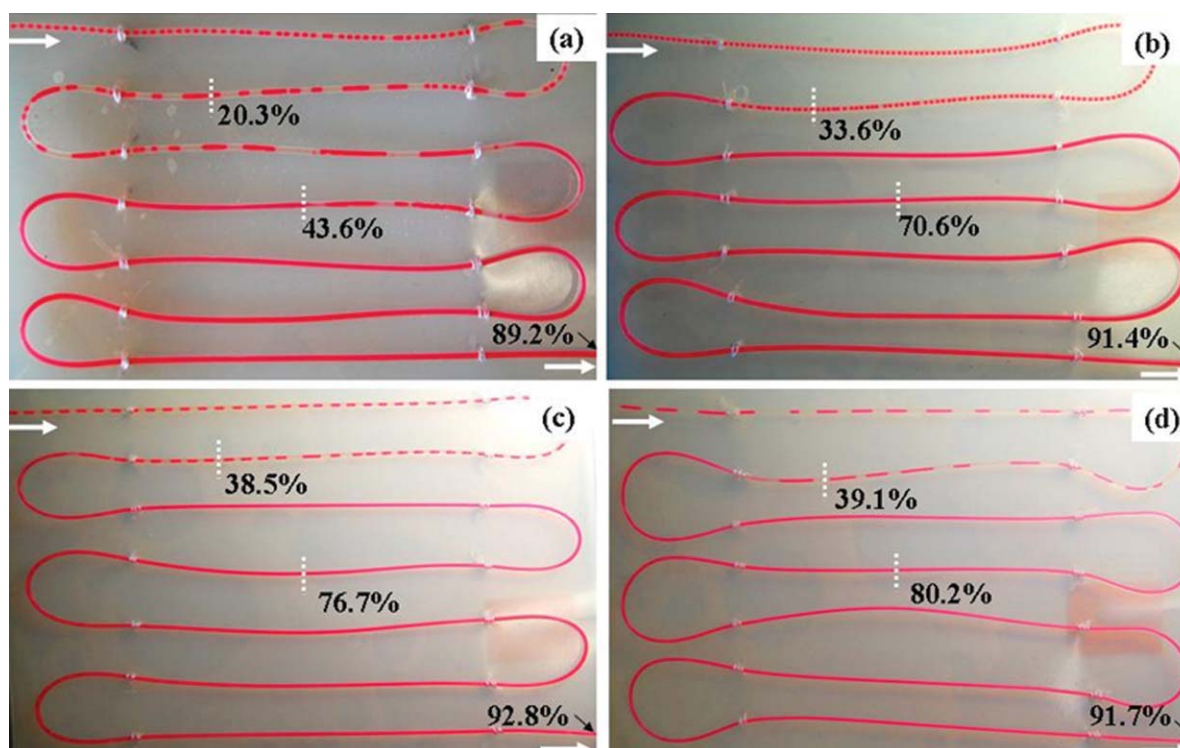


Figure 4. Flow patterns and FAME yield along the flow direction when using WCO for the production of BDF at 333 K in the microtube reactor with different diameters: (a) 0.96 mm; (b) 0.86 mm; (c) 0.68 mm; (d) 0.46 mm.

Residence time = 252 s. [Color figure can be viewed in the online issue, which is available at www.interscience.wiley.com.]

of unreacted oil and methanol. Therefore, the homogeneous phase was formed more easily in the microtube reactor at the final stage of the reaction. In the pendant drop system, most of the FAME could be transported into the large amount of methanol.

Figure 4 shows the flow patterns when using microtubes of different diameters for the transesterification of WCO with methanol at 333 K. The residence time of the reaction mixture in the microtubes was kept constant (252 s at 800 mm away from the inlet). In this case, although the total flow rates for different microtube were set at different value, the flow velocities of the reactants in each microtube were the same. As shown in Figure 4, flow patterns for the four microtubes (0.96, 0.86, 0.68, and 0.46 mm) were similar and changed from separated slug flow through coalescence of slug to parallel flow and then to homogeneous state. However, the elapsed time to a homogeneous state became extended for the 0.96 mm microtube. If the total flow rate was set at the same value, the moving velocities of reactants in different microtube were different, and the smaller the microtube, the faster the moving velocity. In this case, the flow patterns of different microtube were completely different.

The FAME yields along the microtube during transesterification of WCO are also shown in Figure 4. The FAME yield increased with the decrease in the microtube diameter, and the FAME yields reached higher than 89% for all cases at the 800 mm point away from the inlet, corresponding to a residence time of 252 s. When batch reactor experiments were performed for comparisons under 600 rpm at 333 K by

using 100 cm³ flask, FAME yield was 78.3% at a reaction time of 240 s. The homogeneous state in the microtube should be a benefit for the transesterification of WCO due to the enhancement of the mass transfer between oil and methanol. It should be noted that the highest FAME yield from the used WCO in the present study did not exceed 93% even when using a batch reactor with a long enough reaction time at 333 K. As shown in Figure 4, the FAME yields at the points of 800 mm for different microtubes were very close, in the range of 89.2–92.8%, suggesting that the reaction was almost completed for all these microtubes. Although the FAME yield of a 0.46 mm tube at this point was a little bit smaller than that of a 0.68 mm tube, we considered the result an experimental accidental error.

FAME yields as a function of microtube size at the same residence time for different oil feedstock are shown in Figure 5. The residence time of the reaction mixture at the points of 200, 400, and 800 mm in the microtube were 56, 112, and 224 s, respectively. The flow rate ratio of methanol and oil were kept constant for all cases. When the temperature was 313 K, as shown in Figure 5a, the FAME yield decreased with the increase in microtube diameter. This was similar to the results when using a stainless microtube, or FEP tube, in our previous study.²¹ The smaller microtube could be a benefit for heat transfer from the hotplate to the reaction mixtures. Furthermore, as shown in Figure 1, the main flow pattern in this area was the separated slug flow. According to the Young-Laplace equation for the slug flow of a microtube,^{9,28} the pressure drops of oil (ΔP_{oil}) and

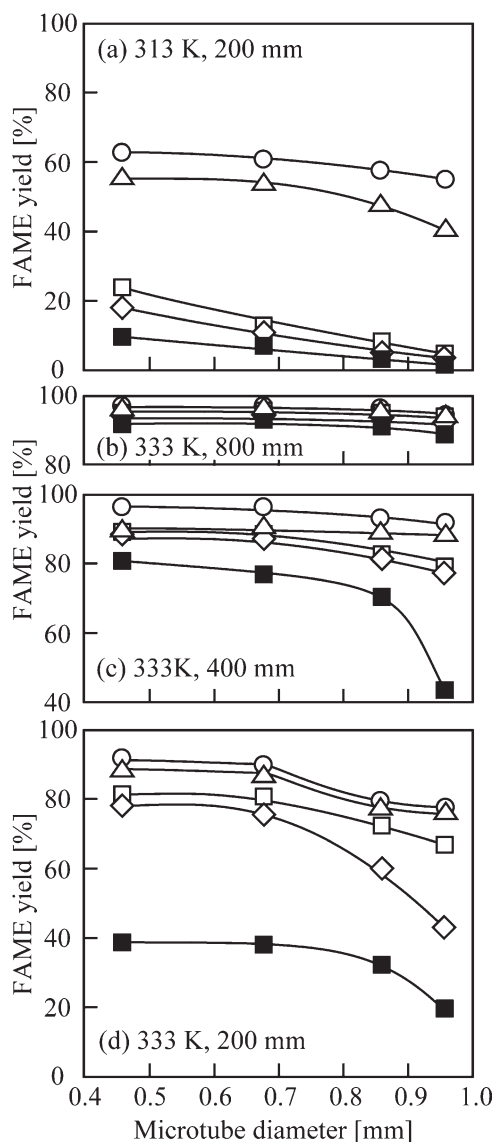


Figure 5. FAME yield as a function of microtube diameter for the oils with different compositions: ○, SFO; △, SFO + 0.8 wt % H₂O; □, SFO + 6.6 wt % oleic acid; ◇, SFO + 0.8 wt % H₂O + 6.6 wt % oleic acid; ■, WCO.

Residence time is the same for each sampling points.

methanol segments ($\Delta P_{\text{methanol}}$) can be calculated using Eqs. 7 and 8, respectively:

$$\Delta P_{\text{oil}} = 16\mu_{\text{oil}}U_{\text{oil}}L_{\text{oil}}/D^2 \quad (7)$$

$$\Delta P_{\text{methanol}} = 16\mu_{\text{methanol}}U_{\text{methanol}}L_{\text{methanol}}/D^2 \quad (8)$$

where D is the diameter of a microtube, μ the liquid viscosity, and L is the total length of the segment. The segment flow velocities of oil (U_{oil}) and methanol (U_{methanol}) are considered to be the same. The total pressure drop ratio in different microtubes was $\Delta P(D = 0.96 \text{ mm}) : \Delta P(D = 0.86 \text{ mm}) : \Delta P(D = 0.68 \text{ mm}) : \Delta P(D = 0.46 \text{ mm}) = 0.23:0.29:0.46:1$. This means that shear forces between the segments and the

tube wall became strong with a decrease in microtube size, and resulted in strong internal circulation within the segments in the entrance region and in enhancement of the reaction rate.

PTFE had a greater affinity for oil than methanol. Accordingly, a thin oil film could be formed around the inner wall of the PTFE tube. The film thickness (h_{film}) could be estimated by Bretherton's law using the following equation^{9,29}

$$h_{\text{film}} = 0.67D(\mu_{\text{oil}}U_{\text{oil}}/\gamma_{\text{oil}})^{2/3} \quad (9)$$

where γ_{oil} is the surface tension of oil. Obviously, with the same flow velocity corresponding to the same residence time in the microtube, the formed film thickness decreased with the decrease in microtube size. Thus, in the radical direction, the mass transfer distance between the two phases decreased with the decrease in microtube size. In this case, the whole surface of the segment takes part in the mass transfer between two phases. For microtubes with different diameters, the specific surface area (S/V_0) of the methanol segment in the absence and presence of the thin film can be expressed as Eqs. 10 and 11, respectively.

$$S/V_0 = 2/L \quad (10)$$

$$S/V_0 = 2/L + 4/D \quad (11)$$

where V_0 and L are the volume and the length of the methanol segment, respectively. From Eq. 11, it is apparent that the specific interfacial area around the segment ($4/D$) increased with a decrease in microtube diameter. As a result, and as indicated in Figure 5a, the mass transfer between the two phases were considered to increase with the increase in the specific interfacial area in the presence of oil film. Kashid and coworkers^{9,10} also found that the volumetric mass-transfer coefficient in PTFE tubes increased with a decrease in the microtube diameter for the liquid-liquid extraction of the nonreactive systems. However, the homogeneous flow formed from the middle region hindered the size effect of the microtubes in this study.

The water in the oil phase could transfer through the interface to the methanol phase, and hinder the reaction to some extent. However, the effect of water on the FAME yield in the microtube was much lower than that of FFA, as shown in Figure 5a. When FFAs existed in the oil, it could also transfer through the interface and react with KOH to form soap immediately. The formation of soap consumed a part of the catalyst in the methanol, and simultaneously hindered the contact of the oil and the methanol. As a result, the FAME yield decreased to a great extent at 313 K.

When the reaction temperature was raised to 333 K, the flow pattern was changed, as shown in Figure 1. The effects of an addition of oleic acid and water to the SFO on the FAME yield at 333 K decreased to some extent, especially for the small microtube as shown in Figure 5d. The FAME yield for WCO was obviously lower than that for SFO containing oleic acid and H₂O because of unknown organic components. The FAME yield reached higher than 89% at the outlet and almost the same value after a residence time of 252 s in the microtube at 333 K for all oils used (Figure 5b). As shown in Figure 1, the shape and the flow state in the slug changed greatly in the region from the inlet to the

point of 400 mm, and as a result, FAME yield increased sharply in this region. For SFO and SFO with water, the transesterification reaction was almost completed at this point. For oil that contained FFA, the flow state was transferred from slug flow to homogeneous flow from a point at 400 to 800 mm. In the homogeneous state, the effect of soap and water should become weaker on the reaction rate. Therefore, the homogeneous flow was a benefit for the completion of transesterification of oil containing FFA in the microtube, particularly in the case of WCO.

Conclusions

Flow patterns in microtube reactors with different diameters during biodiesel production from WCO were investigated in detail. To investigate the effect of FFA and water in the WCO on the flow patterns and FAME yield, oleic acid and/or water were added to SFO. In the case of SFO with FFA and WCO, the presence of FFA greatly changed the flow pattern. No fine droplets containing glycerol and methanol were observed at the interface of the oil and methanol phase at the entrance region. The formation of soap with a strong surfactant property in the presence of FFA could change the interface properties to a great extent, and could hinder the formation of fine droplets in the oil phase. FAME yield along the microtube was greatly influenced by the flow patterns. The formation of a homogeneous flow at the outlet region in the microtube when using the oil with FFA reduces the negative effect of soap and water on the FAME yield. As a result, the FAME yield for the transesterification of WCO reached higher than 89% in microtubes of different sizes with a residence time of 252 s at 333 K.

Acknowledgments

This work was supported by the Research Institute of Innovative Technology for the Earth (RITE) and FWU Grant-in-Aid for Science Research.

Literature Cited

- Hessel V, Löwe H, Müller A, Kolb G. *Chemical Micro Process Engineering—Processing, Applications, and Plants*. Weinheim, Germany: Wiley-VCH, 2005.
- Jähnisch K, Hessel V, Löwe H. Chemistry in microstructured reactors. *Angew Chem Int Ed*. 2004;43:406–446.
- Watts P, Wiles C. Recent advances in synthetic micro reaction technology. *Chem Commun*. 2007:443–467.
- Burns JR, Ramshaw C. Development of a microreactor for chemical production. *Trans IChemE*. 1999;77:206–211.
- Burns JR, Ramshaw C. The intensification of rapid reactions in multiphase systems using slug flow in capillaries. *Lab Chips*. 2001;1:10–15.
- Dessimoz AL, Cavin L, Renken A, Kiwi-Minsker L. Liquid-liquid two phase flow patterns and mass transfer characteristics in rectangular glass microreactors. *Chem Eng Sci*. 2008;63:4035–4044.
- Dummann G, Quittmann U, Gröschel L, Agar DW, Wörz O, Morgenschweis K. The capillary-microreactor: a new reactor concept for the intensification of heat and mass transfer in liquid-liquid reactions. *Catal Today*. 2003;79–80:433–439.
- Kashid MN, Gerlach I, Goetz S, Franzke J, Acker JF, Platte F, Agar DW, Turek S. Internal circulation within the liquid slugs of a liquid-liquid slug-flow capillary microreactor. *Ind Eng Chem Res*. 2005;44:5003–5010.
- Kashid MN, Agar DW. Hydrodynamics of liquid-liquid slug flow capillary microreactor: flow regimes, slug size and pressure drop. *Chem Eng J*. 2007;131:1–13.
- Kashid MN, Harshe YM, Agar DW. Liquid-liquid slug flow in a capillary: an alternative to suspended drop or film contactors. *Ind Eng Chem Res*. 2007;46:8420–8430.
- Malsch D, Kielpinski M, Merthan R, Albert J, Mayer G, Köhler JM, Süße H, Stahl M, Henkel T. μ PIV-analysis of Taylor flow in micro channels. *Chem Eng J*. 2008;135S:166–172.
- Tice JD, Song H, Lyon AD, Ismagilov RF. Formation of droplets and mixing in multiphase microfluidics at low values of the Reynolds and the capillary numbers. *Langmuir*. 2003;19:9127–9133.
- Guan GQ, Kusakabe K, Sakurai N, Moriyama K. Rapid synthesis of biodiesel fuels at room temperature in the presence of dimethyl ether. *Chem Lett*. 2007;36:1408–1409.
- Huber GW, Iborra S, Corma A. Synthesis of transportation fuels from biomass: chemistry, catalysts, and engineering. *Chem Rev*. 2006;106:4044–4098.
- Lotero E, Liu Y, Lopez DE, Suwannakarn K, Bruce DA, Goodwin JG Jr. Synthesis of biodiesel via acid catalysis. *Ind Eng Chem Res*. 2005;44:5353–5363.
- Cater N. Scale up of a more efficient biodiesel process. *Tribol Lubr Technol*. 2004;60:16.
- Cater N. Making biodiesel in a microreactor. *Tribol Lubr Technol*. 2006;62:15.
- Guan GQ, Kusakabe K, Moriyama K, Sakurai N. Continuous production of biodiesel using a microtube reactor. *Chem Eng Trans*. 2008;14:237–244.
- Massingill JL Jr, Patel PN, Guntupalli M, Garret C, Ji C. High efficiency nondispersive reactor for two-phase reactions. *Org Proc Res Dev*. 2008;12:771–777.
- Sun J, Ju J, Ji L, Zhang L, Xu N. Synthesis of biodiesel in capillary microreactors. *Ind Eng Chem Res*. 2008;47:1398–1403.
- Guan GQ, Kusakabe K, Moriyama K, Sakurai N. Transesterification of sunflower oil with methanol in a microtube reactor. *Ind Eng Chem Res*. 2009;48:1357–1363.
- Van Gerpen J, Shanks B, Pruszko R, Clements D, Knothe G. *Biodiesel Analytical Methods*. Colorado: National Renewable Energy Laboratory, 2004:37–47.
- Ambwani DS, Fort T Jr. *Pendant drop technique for measuring liquid boundary tensions*. In: Good RJ, Stromberg RR, editors. *Surface and Colloid Science*, Vol. 11. New York: Plenum, 1979: 93–119.
- Rotenberg Y, Boruvka L, Neumann AW. Determination of surface tension and contact angle from the shapes of axisymmetric fluid interfaces. *J Colloid Interface Sci*. 1983;93:169–183.
- Cerce T, Peter S, Weidner E. Biodiesel-transesterification of biological oils with liquid catalysts: thermodynamic properties of oil-methanol-amine mixtures. *Ind Eng Chem Res*. 2005;44:9535–9541.
- Felice RD, Faveri DD, Andreis PD, Ottonello P. Component distribution between light and heavy phases in biodiesel processes. *Ind Eng Chem Res*. 2008;47:7862–7867.
- Zhou H, Lu H, Liang B. Solubility of multicomponent systems in the biodiesel production by transesterification of *Jatropha curcas* L. oil with methanol. *J Chem Eng Data*. 2006;51:1130–1135.
- Horvolgyi Z, Kiss E, Janos P. Experimental studies on the control of slug flow by interfacial forces in silylated capillaries. *Colloids Surf*. 1991;55:257–270.
- Bico J, Quere D. Liquid trains in a tube. *Europhys Lett*. 2000;51: 546–550.

Manuscript received Mar. 2, 2009, and revision received July 8, 2009.